Brain-Computer Interfaces

ISSN: 2326-263X (Print) 2326-2621 (Online) Journal homepage: http://www.tandfonline.com/loi/tbci20

Continuous affective states recognition using functional near infrared spectroscopy

Dominic Heger, Christian Herff, Felix Putze, Reinhard Mutter & Tanja Schultz

To cite this article: Dominic Heger, Christian Herff, Felix Putze, Reinhard Mutter & Tanja Schultz (2014) Continuous affective states recognition using functional near infrared spectroscopy, Brain-Computer Interfaces, 1:2, 113-125, DOI: 10.1080/2326263X.2014.912884

To link to this article: http://dx.doi.org/10.1080/2326263X.2014.912884

Brain-Computer Interfaces, 2014
Vol. 1, No. 2, 113–125, http://dx.doi.org/10.1080/2326263X.2014.912884

Continuous affective states recognition using functional near infrared spectroscopy

Dominic Heger*, Christian Herff, Felix Putze, Reinhard Mutter and Tanja Schultz

Cognitive Systems Lab, Karlsruhe Institute of Technology, Karlsruhe, Germany

(*Received 22 December 2013; accepted 16 March 2013*)

Monitoring the affective states of a person can be highly relevant for numerous disciplines, including adaptive user interfaces, entertainment, ergonomics, medicine and therapy. In many situations, the affective state of a user is not easily observable from outside by audio or video, but may be identified by a brain-computer interface (BCI). Functional near-infrared spectroscopy (fNIRS) is a brain imaging modality gaining rising attention in the BCI community. However, fNIRS emotion recognition studies have only analyzed stimulus-locked effects. For realistic human-machine interaction scenarios, the point of time of an emotion-triggering event and the time span of an affective state are unknown. In this paper, we investigate a BCI that monitors the affective states of the user continuously over time (i.e. asynchronous BCI). In our study, fNRIS signals from eight subjects have been recorded at eight prefrontal locations in response to three different classes of affect induction by emotional audio-visual stimuli plus a neutral class. Our system evaluates short windows of 5 s length to continuously recognize affective states. We analyze hemodynamic responses, present a careful evaluation of binary classification tasks, compare time-domain and wavelet-based signal features, and investigate classification accuracies over time.

Keywords: functional near-infrared spectroscopy; affect recognition; emotion recognition; continuous; asynchronous; brain-computer interfaces

1. Introduction

Emotions are psycho-physiological processes that play a key role in human life. They are an essential part of social interaction and can have strong regulatory influence on many important conscious and unconscious aspects of human behavior, including influences on perception, learning, and decision-making. Since the 2000s, affective computing [1] has grown into a highly vivid area of research. Many important research questions on affective recognition, modeling, and expression still remain open. It may still be a long way until the vision of intelligent machines that sense human emotions in order to act in a natural, humanlike, and empathic way becomes reality. However, there are some examples in research that have successfully shown that systems adapting to cognitive or affective user states can be advantageous and are preferred by their users (e.g. [2–4]). In addition to that, affective computing technology has strongly contributed to multiple disciplines besides the field of human-machine interaction. For example, emotion-recognition systems have been used in medical applications, such as autism-spectrum disorder therapy (e.g. [5,6]) and, in the future, additional disciplines may benefit from the possibility to continuously monitor a person's affective states, including adaptive user interfaces, biofeedback, psychological research, assessment of the quality of life of patients in clinical settings, entertainment, and ergonomics.

1.1. Affect recognition by brain-computer interfaces

Affective states manifest themselves in various biosignals. However, they originate in different brain circuits that relate to emotions. Besides subcortical areas, such as parts of the limbic system (e.g. amygdala, basal ganglia, and anterior cingulate cortex),[7–11] the essential role of the prefrontal cortex (PFC) in emotion induction and regulation has been shown (e.g. [7,11–13]). The function of the PFC in emotional processing is still not completely clear, but has partly been discovered, for example the strong relation of the orbitofrontal cortex to rewarding stimuli.[7]

For several years, brain-computer interfaces have successfully been developed that provide strongly motor impaired patients a way of communication and control of computing devices. More recently, so-called passive BCIs [14] have gained increasing attention. Instead of using an explicit control intention, they aim at passively observing information about cognitive or affective mental states from the users' brain activity. Several passive BCI systems for monitoring of user states such as attention, workload, and also affective states have been proposed. Most of these systems use electroencephalography (EEG) as the input modality.[15] In the last few years, fNIRS has become more and more popular as a non-invasive measurement technique for BCIs.

*Corresponding author. Email: dominic.heger@kit.edu

1.2. Functional near-infrared spectroscopy (fNIRS)

fNIRS is an optical imaging modality detecting changes in regional cerebral blood flow. According to the blood oxygen level dependent (BOLD) effect, oxygenated (HbO_2) and deoxygenated (HbR) hemoglobin are functional indicators of brain activity. fNIRS exploits the fact that HbO_2 and HbR have different absorption rates for light in the near infrared part of the spectrum. As near infrared light disperses through biological tissue, but is absorbed by hemoglobin, light sources and detector optodes placed on the subjects' scalp can be used for functional brain imaging. Using the modified Beer-Lambert Law [16] changes in the cerebral blood flow, and thereby brain activity, can be estimated from the changes in light intensities. Measurement positions arise roughly in the middle between transmitter and detector at a depth of half the source detector distance. Typically, HbO_2 levels in a cortical area rise with brain activity and peak approximately 5 – 10 s after the beginning of activation. HbR levels should fall in the same intervals. Compared to functional magnet resonance imaging (fMRI), which also measures BOLD responses, fNIRS is comparably cheap, portable, and does not confine the subjects. In comparison to EEG, fNIRS is not susceptible to electrical artifacts from environmental and physiological sources. Furthermore, no conductive gel needs to be used and frontal fNIRS recordings, where measurements are not obstructed by hair, have very short setup times (about 1 min).

1.3. Contributions

In the BCI research community, there is a growing interest in fNIRS as an innovative brain imaging modality. However, there have only been a small number of studies that have analyzed fNIRS in a BCI-typical way, i.e. single-trial processing that is suitable for online applications. In this article, we further explore the advantages and limitations of this measurement technique for affective-state classification by asynchronous BCIs.

This article is an extended version of our workshop paper [17] about our system for the continuous decoding of affective states from fNIRS signals, i.e. decoding affective states continuously over time, instead of evaluating responses that are synchronized to system-controlled stimuli. To the best of our knowledge, other fNIRS studies on emotion recognition have only investigated event-related responses to emotional stimuli using stimulus-locked evaluations. However, such setups are primarily restricted to laboratory conditions as they make the assumption that the point of time of an emotion-triggering event and the time span of an affective state are known. In our evaluation, we investigate whether small chunks (i.e. 5 s) of fNIRS data contain enough information to obtain information about the affective states of a person. Our system classifies such short slices of the fNIRS signal stream and outputs estimates of the affective user state continuously over time. We analyze the binary classification tasks of distinguishing the emotion classes from a neutral class, detecting an emotion class among the other classes, and discriminating the emotion classes pair-wise against each other. In addition to the analyses presented in our previous paper,[17] this article presents an optimized signal processing and compares the classification results of simple time-domain features and more complex time-frequency domain features (Daubechies wavelets). Furthermore, we added an evaluation of affective class detection, i.e. the classification of one affective class versus all other classes. In addition to that, we present a more detailed evaluation of all results. The improvements led to overall increased recognition rates and especially significant results for the discrimination of different affect classes.

1.4. Related work

Numerous systems for the automatic classification of emotions from speech, visual, or biophysiological data have been proposed (see e.g. [18,19] for review). They typically follow a pattern-recognition approach, where features are extracted from preprocessed input signals and classified by machine learning methods. For training data collection, mostly controlled laboratory settings are used. The perception of emotional stimuli has been shown to be an effective method for emotion induction in such experiments. Standardized picture sets and sound samples for emotion induction are available. In numerous studies emotional stimuli based on the International Affective Picture System (IAPS) [20] and International Affective Digital Sounds (IADS) [24] have been used. To quantitatively describe emotions, discrete classes of emotions (e.g. Ekman's basic emotions [21]) or dimensional emotion models (e.g. Russell's Pleasure-Arousal-Dominance scale [22]) are most widely used. IAPS and IADS have been rated using the Self Assessment Manikins scale in the dimensions pleasure, arousal, and dominance by large groups.[23,24]

Several studies investigated fNIRS signals in the context of emotions and showed significant activations of the prefrontal cortex in response to emotionally loaded stimuli. Doi et al. [12] recently conducted a review on fNIRS as a tool for the assessment of emotional function in the prefrontal cortex (PFC). They concluded that fNIRS-based research is highly suitable to quantify several aspects of emotional processing in the PFC, including sensitivity to rewarding stimuli and processing of visceral reactions. Herrmann et al. [25] showed that the prefrontal cortex is activated in response to emotional induction by pictures and facial expressions using fNIRS and investigated these effects with regard to task

requirements. Hoshi et al. [26] found that most subjects showed decreases in HbO_2 in multiple channels during the presentation of pleasant pictures. Half of the subjects showed significant increases of HbO_2 during unpleasant pictures. Morinaga et al. [27] reported activations of HbO_2 in right frontal regions during anticipatory anxiety. Kreplin and Fairclough [28] recently investigated activation of the medial rostral PFC while viewing positive and negative emotional images using fNIRS. They found a significant increase of oxygenated blood during viewing of pleasant pictures, which was shown to be unaffected by two different viewing conditions, namely emotional introspection and spotting differences in the pictures. Further studies reported gender differences in prefrontal activations during emotion induction [29,30] and investigated differences in emotion induction and emotion regulation.[31]

In the last few years, fNIRS-based brain-computer interfaces have been developed that use different task paradigms, including motor imagery, mental arithmetics, mental workload, and speech and language (e.g. [32–37]). To the best of our knowledge Tai and Chau [38] were the first to investigate single-trial recognition of an emotion task. They recorded 16-channel fNIRS from the prefrontal cortex in response to affective induction using emotional images. Their system applied a genetic algorithm to find the optimal analysis interval length, feature set, and classifier. They report recognition rates of 75–97%, investigating to discriminate baseline periods from emotion-induction periods; however, they did not analyze the discrimination between different emotion classes.

Hosseini et al. [39] decoded whether subjects like or dislike different visually presented objects using fNIRS signals recorded from the anterior frontal cortex. Moghimi et al. [40] showed that emotional responses to music can automatically be classified using prefrontal fNIRS signals. They discriminated emotional music from brown noise and emotional valence (positive versus negative) with average recognition accuracies above 70%. Asano et al. [41] induced comfortable and uncomfortable affective states by different sounds (music and scratch sounds). They measured 32 channels of frontal fNIRS and discriminated two affective states using Bayesian nets with an average accuracy of 67%.

2. Material and experimental design

2.1. Participants

Eight healthy male volunteers participated in the experiment (mean age 27.6 ± 5.2 years). All subjects had normal or corrected to normal vision and normal hearing. None of them had a history of brain injury, cardiovascular disease, drugs, or psychiatric conditions. Subjects were instructed about the experiment and provided informed consent before the start of the recordings.

2.2. Stimuli

We composed a slideshow for audio-visual emotional induction containing stimuli from the International Affective Picture System (IAPS) and International Affective Digital Sounds (IADS). Pictures and sounds with extreme ratings in valence and arousal according to the self-assessment ratings in [23,24] were selected and categorized into the following three emotion classes:

- **VA** - Maximum valence and maximum arousal This class contained, for example, pictures of female erotica and exciting sports, rhythmic music, and shouts of joy.
- **Va** - Maximum valence and minimum arousal This class contained, for example, pictures of flowers and animals, calm classical music, and natural and environmental sounds.
- **vA** - Maximum arousal and minimum valence This class contained, for example, pictures of mutilated persons and threatening situations, sounds from an air raid, and screaming persons.

Picture and sound items[1] were selected to induce a strong emotional stimulation during the experiment in order to achieve discriminability between the classes. Similar slideshows for audio-visual emotion induction have successfully been used in one of our previous studies,[42] where subjects rated the stimuli as having a strong emotional impact corresponding to the emotion classes in terms of valence and arousal (self-assessments). Table 1 summarizes average subjective ratings of the pictures and sounds used in the experiment.

2.3. Experimental procedure

Affective pictures were presented on a computer screen located at about 0.5 m distance, while subjects were sitting in a comfortable office chair. Sounds were played using headphones at a moderate volume that was set identical for all subjects. Each subject was instructed just to watch the slideshow and to avoid unnecessary movements.

During one recording session subjects attended 30 emotion induction blocks (i.e. 10 blocks for each of the emotion classes **VA**, **Va**, **vA**) of 35 s length. Each block contained 4 or 5 images and 4–8 sound samples. The order of the blocks and the selection of pictures and sounds was pseudorandomized. A neutral blank screen was displayed and no sounds were played for 30–40 s after each block and at the beginning of the experiment (called **Neutral** throughout the paper). The duration of the **Neutral** phases was randomly varied between 30 and 40 s to reduce a potential systematic influence of slow waves. The total recording time of one recording session was about 35 min. Figure 1 summarizes the experiment procedure.

Table 1. Subjective ratings according to [23] and [24] of the selected pictures and sounds of the three emotion classes. Means (standard deviations) on a 9-point scale.

	IAPS		IADS	
Emotion class	Valence	Arousal	Valence	Arousal
VA	7.48 (1.42)	6.94 (1.88)	7.13 (1.79)	6.95 (1.80)
vA	2.25 (1.49)	6.17 (2.31)	2.41 (1.61)	7.29 (1.81)
Va	6.71 (1.58)	3.49 (2.10)	6.31 (1.66)	4.14 (2.06)

2.4. *fNIRS measurement*

To measure cerebral hemodynamics we used an Oxymon Mk III system from Artinis Medical Systems. The montage consists of four transmitter and four detector optodes. The optodes were attached to the subjects' foreheads using a headgear, so that its lower edge was shortly above the eyebrows and the optodes were symmetrical to the head midline. Figure 2 illustrates the optode montage. Using this setup, the system measures concentration changes in oxygenated (HbO_2) and deoxygenated (HbR) hemoglobin at eight source-detector pairs (16 channels) at a distance of 3.5 cm using a sampling rate of 25 Hz. To assess exact timings of the pictures synchronously with the fNIRS data, a light-intensity sensor was attached to the screen and connected to an AUX input of the Oxymon system.

3. Methods

3.1. *Signal-processing artifact removal and windowing*

The measured fNIRS signals are usually subject to biological and technical artifacts. Mostly influences from cardiovascular activity, such as heart beats and slow waves (e.g. Mayer waves) as well as spikes caused by optode movements are present in the recorded signals (see e.g. [43,44] for more detailed information on artifacts in fNIRS). To remove signal drifts and slow waves, we applied an elliptic IIR high-pass filter with cutoff frequency 0.006 Hz (filter order 6). We applied an elliptic IIR low-pass filter with cutoff frequency 0.5 Hz (filter order 5) to remove higher-frequency influences, including heart beat. Movement artifacts and spikes were removed using the wavelet based method proposed by [45].

In order to continuously classify affective states, windows of 5 s length with 50% overlap were extracted from the preprocessed fNIRS signals. This setup appears to be short enough to have a sufficient time resolution for many applications and appears to be long enough to extract stable and discriminative features from the fNIRS signals. Preliminary evaluations using the signal mean as features showed that window lengths up to 15 s appeared to give rather similar results and longer windows tended to be more unstable. This can be explained by the block length of 35 s and the small amount of data available.

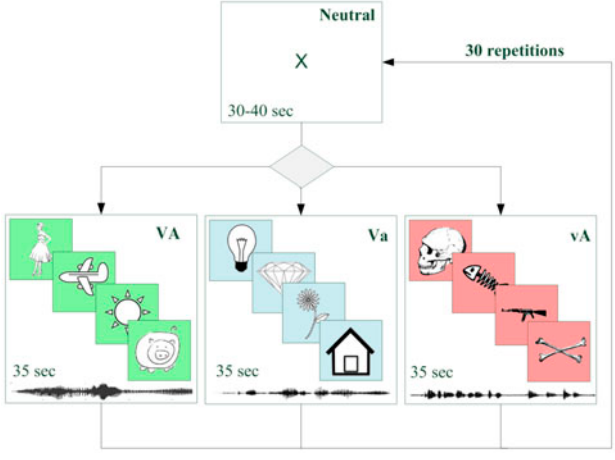

Figure 1. (Color online) Experimental protocol for data collection consisting of three different emotion induction blocks **VA**, **vA**, **Va**, and **Neutral** blocks.

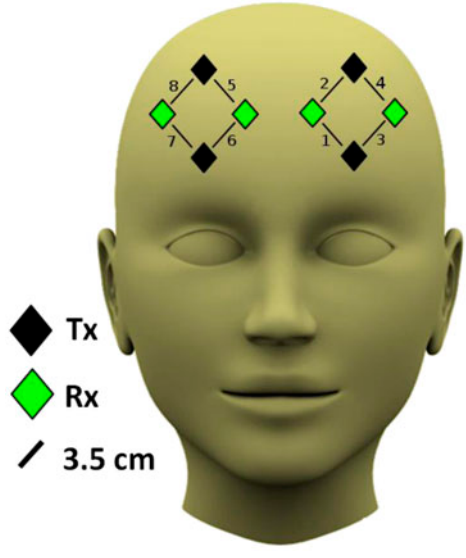

Figure 2. (Color online) Optode montage used in the experiment. Tx stands for transmitters, Rx for detector optodes. The optode distance is 3.5 cm for all measurement locations.

Using this procedure, 14 windows were recorded for each of the 10 emotion blocks and each emotion class (**VA**, **Va**, or **vA**) during one session (35 s block length, 2.5 s shift). The length of **Neutral** blocks was 30–40 s which corresponds to 12–16 windows. Each window was associated with its best-fitting class label (**Neutral**, **VA**, **Va**, or **vA**). The following section describes the feature extraction that transforms each window into one example (feature vector) that can be used for either training or testing of the continuous affect-recognition system.

3.2. *Feature extraction*

Several different feature-extraction methods have been used for fNIRS-based BCIs, including simple statistical properties of the time-domain signals, such as mean, standard deviation, slope, kurtosis, and skewness. These features intuitively express properties of the characteristic shape of a hemodynamic response when applied to stimulus-locked fNIRS signals. However, in the case of continuous recognition, the signal properties that these features reflect are not interpretable as easily.

For the evaluations in this paper, we decided to use features based on the signal mean and compare the results to features based on time-frequency analyses (i.e. discrete wavelet transformations), which are more complex and may reflect additional signal properties. In previous studies [38,40], the mean was among the most successful features to discriminate fNIRS signals in emotion tasks; however, wavelet-based features have regularly been used to denoise and analyze fNIRS data and have shown good performance in other fNIRS classification tasks.[45–48]

3.2.1. *Mean feature calculation*

Mean features were calculated for each extracted window of 5 s length, i.e. the mean values of each of the eight HbO_2 and eight HbR signal chunks were stacked to a 16-dimensional feature vector.

3.2.2. *Wavelet feature calculation*

Discrete wavelet transform (DWT) based features were calculated using the multi-resolution analysis [49] algorithm, which iteratively decomposes the original signal into different scales of resolution. The algorithm convolves the signal with low-pass and high-pass wavelet decomposition filters and subsamples the result by factor 2 to obtain an approximation component (low-frequency coefficients) and a detail component (high-frequency coefficients). This decomposition step is iteratively applied to the approximation components, i.e. the approximation component is the input signal for the next decomposition level, which results in a binary tree of an approximation and a detailed component at each level. The maximum depth of the tree is determined by the length of the input signal and the length of the wavelet filters. Due to the downsampling, the corresponding frequency band for the approximation and detail components can be calculated. Approximation coefficients correspond to the frequency range $[0 - {}^{s}/_{2^{level+1}}]$ Hz and detail coefficients correspond to $[{}^{s}/_{2^{level+1}} - {}^{s}/_{2^{level}}]$ Hz, where s is the sampling rate.

There is a rich family of different wavelets that have been used to analyze fNIRS signals. One of the most popular types of wavelets is Daubechies wavelets.[50] We evaluated Daubechies wavelets (DBN) for different numbers N of vanishing moments ($N \in [1,\ldots,10]$) and decided to use $N = 3$ for the evaluations in this paper. The recognition results of Daubechies wavelets with $N < 7$ vanishing moments appeared to give similar performance, whereas wavelets with more vanishing moments had lower performance, which might be explained by the fact that only decompositions to two or three levels have enough coefficients to allow a correct convolution with respect to the length of the wavelet filters.

Since we expect the relevant information mostly in the fNIRS signals mainly below 1 Hz, we used features that correspond approximately to the frequency band 0~0.78 Hz by decomposing the 5 s windows (sampled at 25 Hz) into four levels and using the approximation coefficients as features. This results in four coefficients per channel, which are stacked for the final feature vector. Including detailed coefficients did not increase recognition performance.

3.2.3. *Feature selection*

We filtered out features that contained only little information using a mutual information-based feature selection (similar to the mutual information best individual feature approach in [51]). For this purpose, mutual information between the continuous training data of each feature and the corresponding discrete emotion class labels (ground truth) was calculated, using non-parametric probability density functions estimated by kernel density estimation (Parzen windows). Features that contributed less than 10% to the total mutual information in the training data were excluded from the feature vector, which results on average in 11.7 (std. 1.2) of 16 features for the mean features and 44.6 (std. 4.3) of 64 features for the wavelet-based features.

3.3. *Continuous affect classification*

As the amount of data available to train and test the system is very limited, we decided to use 10-fold cross-validations for the classification performance evaluations

of our system. Using this evaluation scheme, one has to be careful that no hidden information from the test data is used for training, otherwise the performance will be overestimated. In addition to that, the high temporal auto-correlation of fNIRS signals makes it problematic to include examples very shortly before or after the examples to be predicted in training, as neighboring training examples contain nearly the same information (e.g. this makes common evaluation schemes including random shuffling inappropriate).

In our cross-validation experiments we split the data chronologically and ensured that examples 30 s before and after the testing examples were not included in training (i.e. training examples were ignored). In each fold of the cross-validation the training data were balanced to an equal number of examples for both classes, in order to avoid a bias of the classifier towards one class. Balancing was done by removing random examples from the training data. The mutual information-based feature selection was performed on the training data in each fold of the cross-validation. For the evaluations in this paper we used Fisher's linear discriminants (LDA) to classify the data. Using LDA instead of support vector machines (as used in our previous paper [17]) has the advantage of faster processing as no hyper-parameters have to be estimated using nested cross-validations; furthermore LDA can achieve similar recognition rates.

4. Results and discussion

4.1. Hemodynamic responses to the emotion induction

In order to analyze the hemodynamic responses to the four different classes during emotion elicitation, we extracted stimulus-locked epochs starting 5 s before the beginning of an emotion induction block until 10 s after each emotion block. Figure 3 shows grand averages of the hemodynamic responses after applying the preprocessing as described in section 3.1. Each plot in the upper row shows HbO_2 channels; the plots in the lower row show HbR channels averaged across subjects. The columns correspond to the classes **VA**, **vA**, **Va**, and **Neutral**, respectively.

Hemodynamic responses to the emotion induction are strongly pronounced and show a typical shape in all channels and all classes. For the three emotion classes (**VA**, **vA,** and **Va**), HbO_2 channels show an increase (hyper-oxygenation), while HbR channels show a slight decrease in concentration a few seconds delayed after the beginning of each block. One can see that the hemodynamic responses remain stable for the complete time of the emotion induction (block length 35 s) and turn towards baseline after the end of an emotion-induction block. A contrary effect can be observed for the **Neutral** plots, i.e. HbO_2 decrease and HbR increase after the beginning of the block. This can be explained by a recovery effect, since **Neutral** blocks occur directly after the emotion-induction blocks and include the decay of the hemodynamic activity.

Figure 4 shows HbO_2 and HbR signals of all emotion-induction blocks (30 blocks per subject stacked) at all channel locations. The overall hemodynamic activation pattern can be recognized at all recorded locations. Apart from that, there are no obvious topographical patterns, such as lateralization effects, that can consistently be observed for all subjects.

4.2. Continuous affect recognition performance

To quantify the performance of our affect recognizer, we evaluated three types of binary classification experiments:

- Discriminating the affective classes (**VA**, **vA**, **Va**) versus **Neutral**
- Detectors for the affective classes (**VA** versus {**Neutral** ∪ **Va** ∪ **vA**}, **vA** versus {**Neutral** ∪ **Va** ∪ **VA**}, **Va** versus {**Neutral** ∪ **VA** ∪ **vA**}, **Neutral** versus {**VA** ∪ **Va** ∪ **vA**})
- Discriminating the affective classes against each other (**VA** versus **Va**, **Va** versus **VA**, **VA** versus **vA**)

Figure 5 shows classification accuracies averaged across subjects for the corresponding binary classification tasks using mean and Daubechies 3 wavelet (DB3) based features. The results were calculated using 10-fold cross-validation with a 30 s gap before and after test set examples. The error bars indicate standard deviations across subjects. We calculated one-sided Wilcoxon signed rank tests to test whether the recognition accuracies are significantly ($p < 0.05$) above the 50% chance level. All results in Figure 5 were significant (with the only exception of **Va** vs. **vA** for mean features). Table 2 lists the corresponding individual subject accuracies for both mean and DB3 features for each classification task.

We also evaluated the results on subject level, i.e. Wilcoxon signed rank tests on the results of the 10 folds of the cross-validation for each subject. Variances across the different folds of the cross-validation were in general higher than those of cross-validation results between subjects. Nonetheless, almost all of the classification tasks discriminating the affective classes from **Neutral** were significant for all subjects. Similar results can be observed for the affective class detection tasks. For discriminating **Va** against **VA** the results of nearly all subjects were not significantly above chance level using Wilcoxon signed rank tests on subject level. This might be explained by the fact that these classes are most

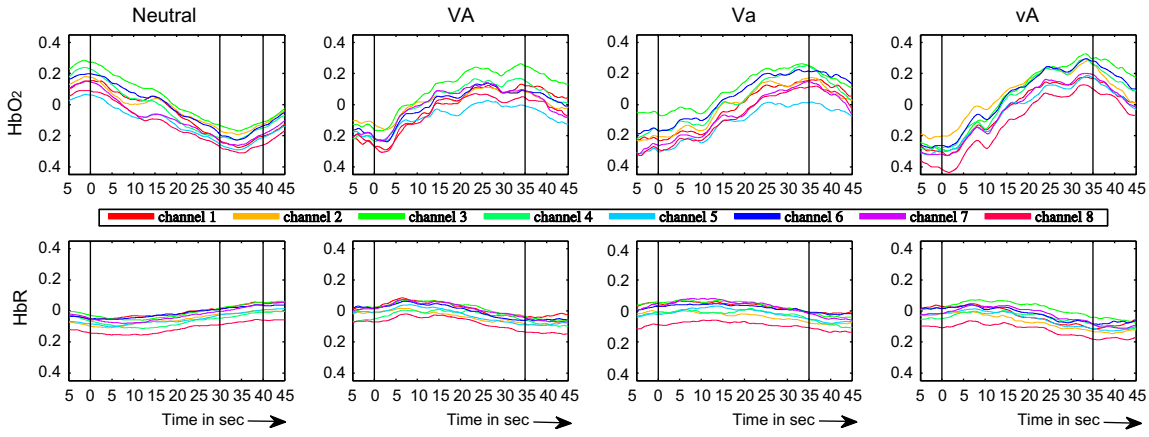

Figure 3. (Color online) Hemodynamic responses (grand averages) for the classes **VA**, **vA**, **Va**, and **Neutral**. The top row shows HbO_2 channels, the bottom row shows HbR channels. Signal epochs start 5 s before the beginning of an emotion induction or **Neutral** block and end 10 s after the end of the blocks. Vertical lines indicate beginning and end of a block (as **Neutral** blocks have random length, the second and third vertical lines in these plots indicate the time when the blocks end). The *x*-axes show time in seconds; the *y*-axes show concentration changes of HbO_2 and HbR.

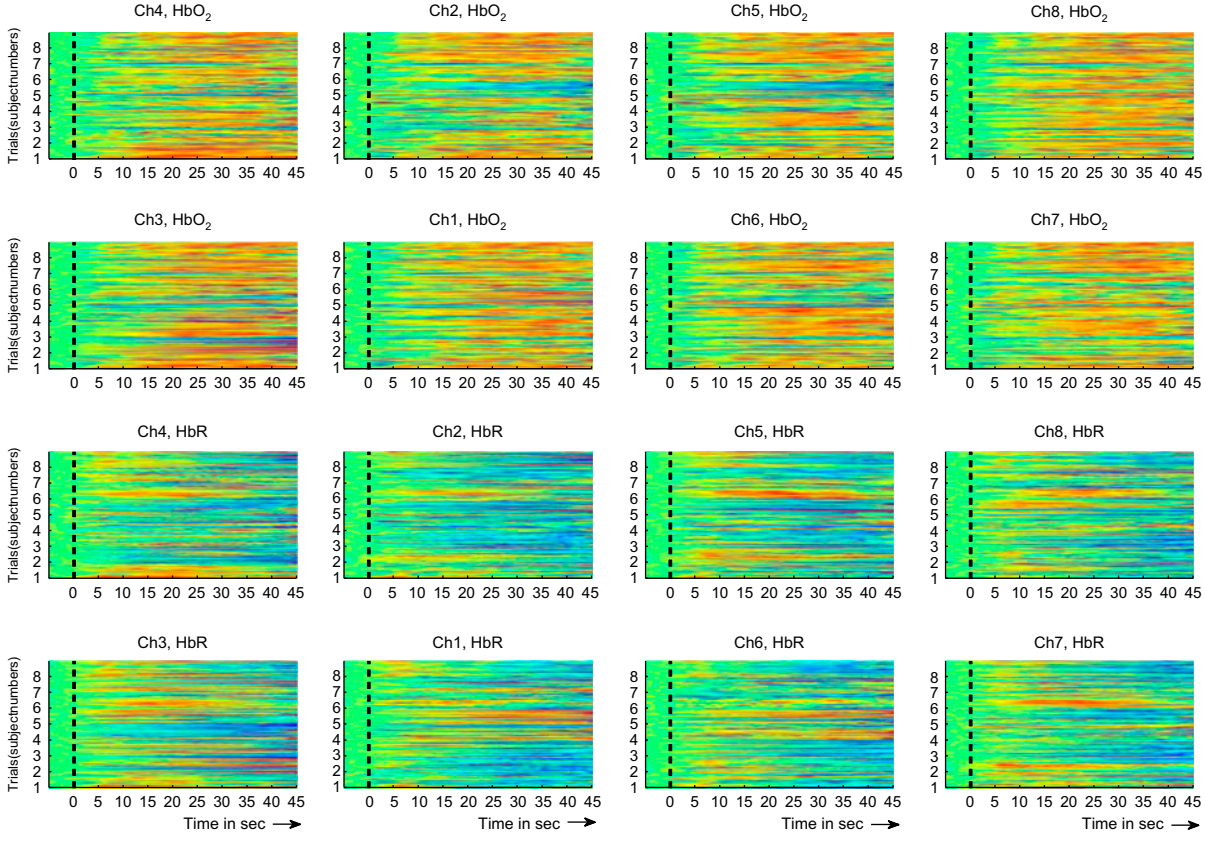

Figure 4. (Color online) Each plots shows HbO_2 and HbR signals of all emotion-induction blocks (30 blocks per subject stacked) at a specific channel location. Plots are arranged corresponding to the recording location (i.e. left plots show left head locations).

similar according to the valence and arousal ratings in Table 1. For discriminating **Va** versus **vA** and **VA** versus **vA** the results for the mean features include three significant subjects, whereas using the DB3 features the recognition rates of five subjects were significantly above chance level.

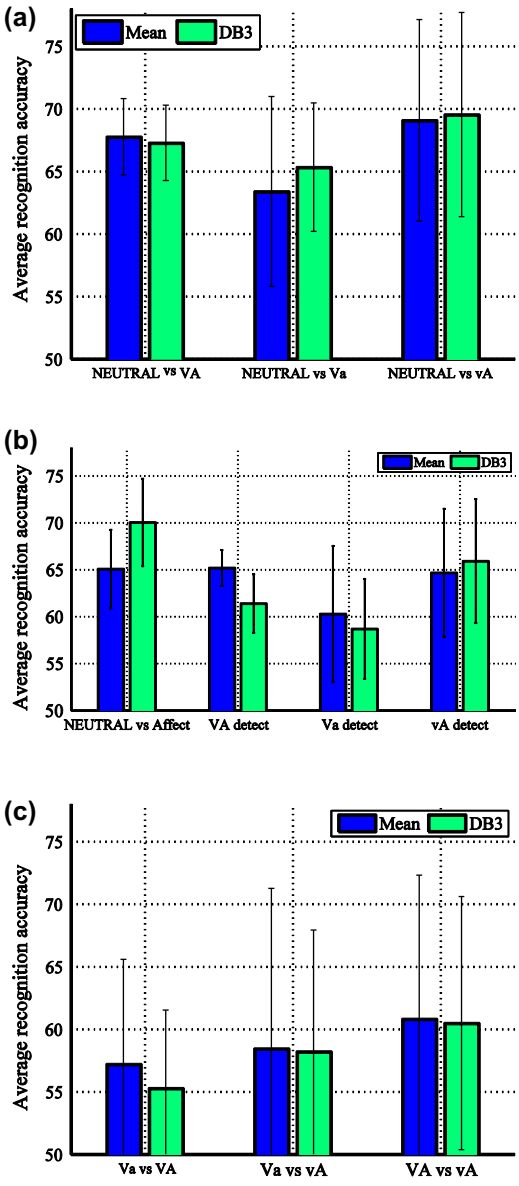

Figure 5. (Color online) Cross-validation results averaged across subjects for all classification tasks using mean and Daubechies wavelet (DB3) features. (a) shows affective classes versus Neutral, (b) affective class detection, and (c) discriminating affective classes against each other. Error bars indicate standard deviations across subjects.

Since the autocorrelation of the fNIRS signal is high and overlapping windows were used, the tested examples may not be completely independent. This can lead to an underestimation of the actual chance level. Therefore, we performed permutation tests, i.e. evaluating the recognition results using 1000 times randomly scrambled ground truth labels as described in section 3.3. As an estimate of the actual chance level we calculated the 95% quantile of the permutation test results. The estimated chance levels for the different classification experiments ranged from 52.0% to 56.4% (mean 54.3%, std. 1.2%). Stars in Table 2 indicate results of recognizing the actual label sequences that are better than the chance level estimated by the corresponding permutation test.

To investigate the results in more detail, Figure 6 shows confusion matrices (accumulated over all subjects) for the different classification tasks. Figure 6a shows the results for mean feature extraction, and Figure 6b shows the results for DB3 feature extraction. All confusion matrices have been normalized by the actual number of instances of the particular class, i.e. values in diagonal elements correspond to the true positive rates (recall) and counterdiagonal values correspond to percentages of false negative classifications (miss rate). For each result and each class, we calculated f-scores, i.e. the harmonic mean of precision (number of correct predictions of the class divided by the number of all predictions for the class) and recall (number of correct predictions of the class divided by the actual number of occurrences of the class). Again, one-sided Wilcoxon signed rank tests were calculated to test whether the f-score results of the cross-validation are significantly above chance level across the eight subjects. Significant recall scores are indicated by a star in the diagonal elements of the confusion matrices in Figure 6. Significant f-scores are indicated by a hash sign.

Comparing the results of the mean features and DB3 features one can see that the number of significant recall scores and f-scores is higher for the DB3 features than for the mean-based features. We calculated (paired) two-sided Wilcoxon signed rank tests on the f-scores. For discriminating **Neutral** against all affective classes, DB3 wavelets performed significantly better than mean features of both classes. In the other tests, with the exception of the detection of 'not **VA**', no significant differences between the two features were shown.

4.3. *Recognition performance over time*

To analyze the continuous affect recognition performance in more detail, we calculated average recognition rates as a function of the time distance from the start of the corresponding emotion-induction block. For this analysis the predictions from the cross-validation experiments were used (as described in the previous section). The time of each emotion induction and **Neutral** block was split into analysis intervals of 5 s length overlapping 4.5 s. Recognition accuracies were calculated using the predictions that occurred within each analysis interval (averaged across subjects). Figure 7 shows the resulting curves of all classification tasks using DB3 features (for mean features a similar plot can be shown, as in our previous paper [17]). The *x*-axis shows the start time of the analysis intervals based on the beginning of the corresponding emotion induction block.

All binary classification tasks show an increase in recognition accuracies after the beginning of emotion

Table 2. Individual subject recognition accuracies for mean-based and Daubechies 3 wavelet-based features. Stars indicate results better than the corresponding estimated chance level performance (95% quantile of permutation test results using 1000 iterations of randomly scrambled ground truth labels).

	Subject							
Task	**1**	**2**	**3**	**4**	**5**	**6**	**7**	**8**
Mean-based features								
Neutral vs. VA	65.8%*	67.1%*	73.1%*	64.8%*	64.2%*	68.8%*	67.2%*	70.9%*
Neutral vs. Va	59.6%*	74.5%*	66.7%*	50.0%	66.2%*	56.7%*	65.2%*	67.9%*
Neutral vs. vA	70.4%*	65.1%*	74.0%*	59.3%*	72.8%*	57.9%*	70.7%*	82.3%*
Neutral vs. Affect	65.6%*	64.4%*	68.8%*	59.0%*	60.9%*	62.9%*	67.2%*	71.7%*
VA detect	66.5%*	61.5%*	67.1%*	65.2%*	65.8%*	66.4%*	65.8%*	63.1%*
Va detect	57.2%*	68.0%*	60.1%*	44.4%	63.3%*	60.2%*	63.1%*	65.8%*
vA detect	65.5%*	64.5%*	65.1%*	57.0%*	75.5%*	53.5%*	69.0%*	67.3%*
Va vs. VA	46.4%	58.2%*	57.9%*	45.7%	52.5%	63.6%*	65.7%*	67.5%*
Va vs. vA	53.9%	67.9%*	58.5%*	29.3%	68.2%*	59.3%*	64.6%*	65.7%*
VA vs. vA	66.4%*	59.6%*	58.9%*	45.6%	81.1%*	48.1%	57.4%*	69.3%*
Daubechies 3 wavelet-based features								
Neutral vs. VA	70.2%*	65.2%*	69.1%*	65.7%*	64.9%*	62.6%*	70.2%*	70.2%*
Neutral vs. Va	63.9%*	75.0%*	61.7%*	57.2%*	66.9%*	64.0%*	66.0%*	67.8%*
Neutral vs. vA	72.3%*	58.9%*	74.2%*	61.2%*	77.4%*	59.5%*	75.6%*	77.0%*
Neutral vs. Affect	74.3%*	65.6%*	75.5%*	68.3%*	68.1%*	62.8%*	70.8%*	75.0%*
VA detect	65.1%*	59.9%*	65.9%*	61.4%*	63.1%*	57.7%*	63.8%*	64.3%*
Va detect	57.9%*	65.1%*	62.3%*	50.6%	62.3%*	61.2%*	57.6%*	66.4%*
vA detect	68.4%*	61.0%*	65.6%*	57.4%*	74.4%*	57.9%*	73.5%*	69.1%*
Va vs. VA	52.5%	52.5%	53.6%	55.0%	47.1%	60.4%*	53.2%	67.9%*
Va vs. vA	53.2%	67.9%*	55.6%	37.9%	64.6%*	60.7%*	66.8%*	58.9%*
VA vs. vA	62.9%*	58.5%*	57.0%*	50.0%	79.3%*	47.0%	61.5%*	67.5%*

induction. Recognition rates for **Neutral** versus **VA** and **Neutral** versus **Va** show a down trend starting at 10-15 s. This appears not to be supported by the plots in Figure 3; however, as **Neutral** blocks occur directly before and after emotion blocks in the experiment, the hemodynamic activity is expected to be similar. This indicates that discriminating the two classes for analysis intervals near the borders of the blocks is more difficult. In all of the other recognition tasks the performance increased and remained rather stable. This analysis shows that the recognition results were not caused by short peaks after the emotion-triggering event; instead, the continuous affective state classification using small windows is effective for classifying longer affective state periods. The peak values of the curves indicate that an optimal analysis interval would have increased average recognition rates well above those reported in Figure 5 for stimulus-locked evaluations. In such a case, the use of specialized classifiers, such as a temporally sliding ensemble classifier,[52] might strongly improve classification performance.

4.4. Influences on the continuous affect recognition

4.4.1. Perceptual properties

When analyzing affective reactions to emotional stimulation based on brain activity, low-level sensory processing may have an influence on the measured signals. Even in rather controlled experimental setups as in our experiment, stimuli are rich in perceptual properties, including differences in sound intensity, sound frequencies, clutter, contrast, and color intensity. It is thus very difficult to balance all properties between the different classes. We checked for differences in the power of the audio signal between blocks for the different classes using Wilcoxon rank sum tests. The results indicate no significant difference for **Va** versus **VA** and **VA** versus **vA**, but a significant difference for **Va** versus **vA** ($p < 0.05$). Nonetheless, we do not expect differences in such activity to have a major influence on the recognition results. This is also supported by [53], who found that there is no significant effect in the BOLD response when pictures are presented in color or in grayscale, and by [28], who found that the increase of oxygenated blood while viewing pleasant pictures is not affected by different viewing conditions. Subjects reported the emotional stimulation to be the primary effect during the experiment. Furthermore, we do not expect cerebral blood flow at frontal regions to be affected by low-level sensory processing, as the primary locations of low-level sensory processing are in the temporal cortex areas for auditory processing and in occipital areas for visual processing.[54,55] Nonetheless, for the tasks of discriminating **Neutral** versus emotion stimulation, there are obviously strong differences in the perceptual properties between the two classes and influences other than affective processing may also have an effect

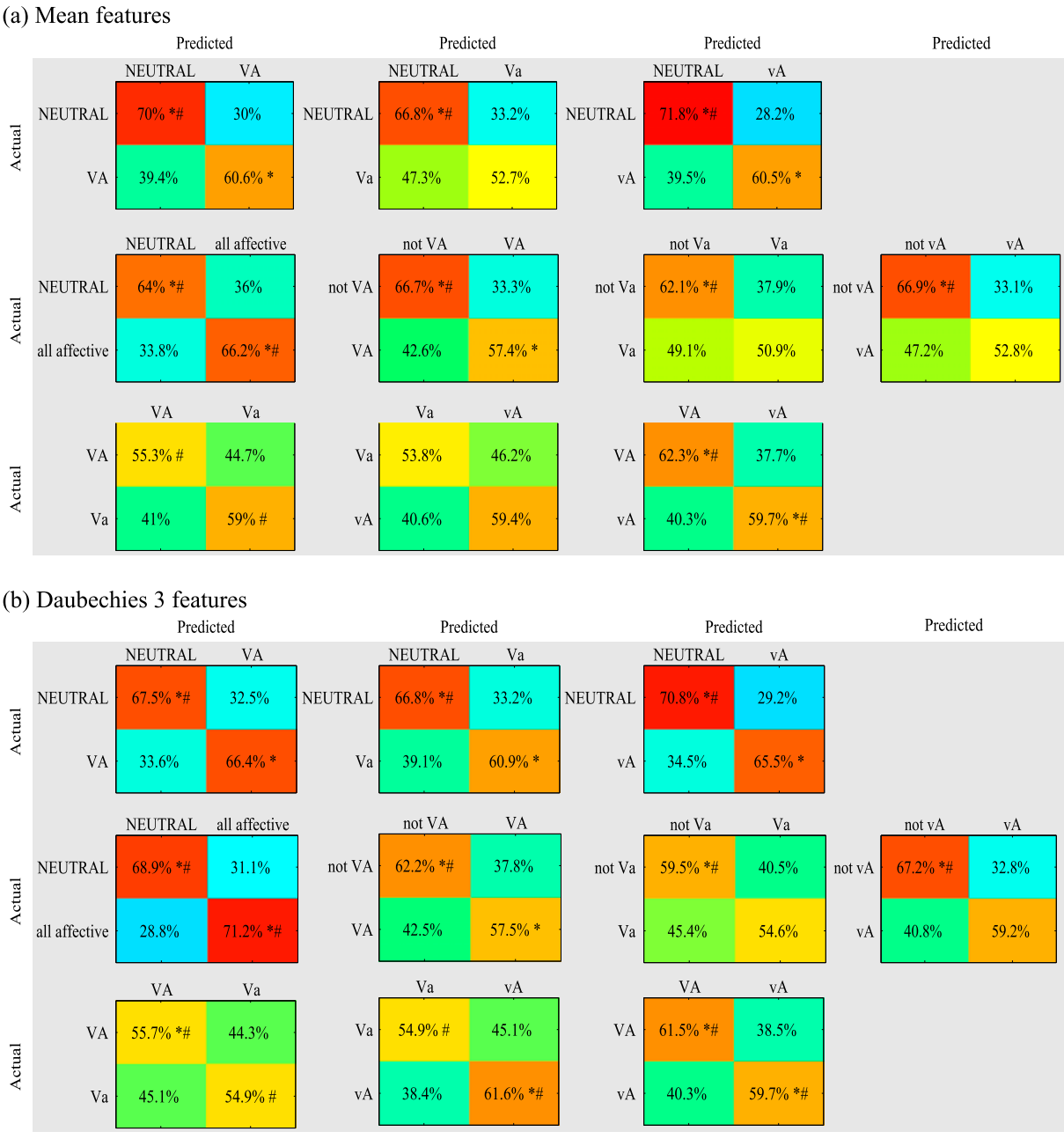

Figure 6. (Color online) Confusion matrices (accumulated over all subjects). (a) Mean-based feature extraction, (b) Daubechies wavelet-based feature extraction. Stars at diagonal elements indicate significant recall scores, hashes at diagonal elements indicate significant f-scores ($p < 0.05$).

on parts of the measured cerebral blood flow, including differences in general activation or relaxation.

Additionally, we want to note that stimuli were presented during the experiment in pseudorandomized order, therefore some pictures and sounds were presented multiple times during the experiment. However, one should note that the content of some of the selected IAPS/IADS stimuli is already very similar, which makes them even hard to distinguish for the subjects (e.g. IADS items 279 and 285: a woman screaming because of fear or pain). Nonetheless, the stimuli were rated to have a strong emotional impact.[24] The reasoning behind our choice of stimuli was to select only stimuli from IAPS/IADS that are among those with the most extreme ratings in terms of valence and arousal.

4.4.2. *Sequence and recovery effects*

We analyzed sequence effects, i.e. the influence of the previous block label on the recognition results, as the

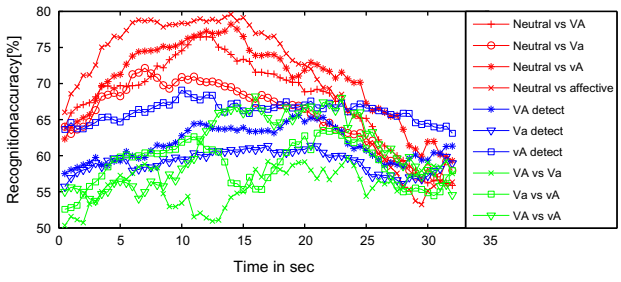

Figure 7. (Color online) Classification accuracies of Daubechies wavelet-based features as a function of the time distance from the start of an emotion induction block. The *x*-axis shows time offset in seconds; the *y*-axis shows average recognition accuracies.

hemodynamic responses of the **Neutral** blocks in Figure 3 indicate a gradual decline that may be caused by the previous emotion induction block. Therefore, the classification accuracies of **Neutral** depending on the class of the previous emotion block were tested pairwise. None of the Wilcoxon rank sum tests showed significant differences ($p > 0.05$). Nonetheless, as indicated by the classification results over time (section 4.3), the recovery effect during **Neutral** blocks may have an influence on the recognition results of the classification tasks discriminating against **Neutral** blocks. To quantify and avoid such effects, additional resting blocks should be recorded during the experiment.

4.4.3. Cardiovascular activity

Due to the strong coupling of the fNIRS measures and the cardiovascular activity, we analyzed differences in heart rate during the different emotion-induction blocks. Oscillatory activity caused by heart beats is clearly visible in the unfiltered fNIRS signals. To obtain an estimate of heart rate for each emotion induction and each **Neutral** block, we calculated power spectral density estimates of each HbO_2 signal using Welch's method and extracted the peak frequencies in the range 0.83–2.67 Hz (which approximately corresponds to 50 to 160 beats per minute). The median of all channels' peak frequencies was used as the heart-rate estimate. We analyzed the heart-rate estimates of each block to see whether there are differences between the classes. Wilcoxon rank sum tests did not show significant ($p < 0.05$) differences between the **Neutral** and each emotion class with the exception of subject 3 for **Neutral** versus **vA**. Therefore, we do not expect cardiovascular effects to have a systematic influence on the results.

5. Conclusions

In this paper, we presented a system for the continuous (i.e. asynchronous) recognition of affective states from fNIRS signals in response to different classes of audio-visual affective stimulation. Continuous recognition is a challenging task and recognition results are expected to be below those of stimulus-locked evaluations. In this study, we chose a simple setup that allows an easy analysis and interpretation of all processing steps involved. The recognition results indicate that it is possible to discriminate Neutral signals from signals recorded during emotion induction, but also to detect different affective states and discriminate different affective classes against each other. We compared simple mean features and more advanced Daubechies 3 wavelet-based features, with the Daubechies-based features being preferable in terms of recall scores and f-scores. The analysis of classification performance over time indicates that the continuous recognition of affective states of longer duration (such as mood) might be possible since recognition rates appear to remain stable for most of the evaluated binary classification tasks. However, this should be verified by further studies that, for example, include emotion induction blocks of different lengths.

In future work, an optimal optode montage should be identified that covers all relevant frontal regions and other brain areas that may contribute additional information. Furthermore, it is important to further improve the recognition performance. This could be achieved by increasing the amount of data and using individual optimizations for each subject. Finally, the system should be evaluated in an online application.

Note

1. The following IAPS picture items have been used:
   VA: 4001, 4002, 4003, 4006, 4141, 4142, 4150, 4180, 4220, 4225, 4232, 4235, 4250, 4255, 4274, 4275, 4279, 4290, 4300, 4310, 4311, 4607, 4608, 4651, 4652, 4659, 4660, 4664, 4670, 4683, 4694, 4695, 4800, 8030, 8080, 8185, 8400, 8501; **Va**: 1440, 1441, 1460, 1560, 1590, 1600, 1601, 1602, 1603, 1604, 1610, 1620, 1640, 1670, 1900, 2000, 2050, 2070, 2170, 2260, 2304, 2341, 2360, 2370, 2501, 5000, 5010, 5020, 5030, 5200, 5551, 5720, 5760, 5800, 5891, 7080, 7325, 7545, 7900; **vA**: 3000, 3010, 3015, 3030, 3051, 3053, 3060, 3062, 3063, 3068, 3069, 3071, 3080, 3101, 3102, 3110, 3120, 3160, 3168, 3170, 3181, 3250, 3261, 3266, 3301, 3400, 3500, 3530, 6230, 6260, 6313, 6510, 6540, 9400, 9405, 9410, 9433, 9570, 9635.1, 9810
   The following IADS sound items have been used:
   VA: 201, 202, 311, 215, 815, 716, 360, 200, 366, 717, 817, 205, 352, 367, 415, 204, 353, 216, 110, 355; **Va**: 112, 150, 151, 171, 172, 230, 262, 270, 370, 374, 377, 602, 705, 721, 725, 726, 809, 810, 811, 812; **vA**: 115, 260, 275, 276, 277, 278, 279, 284, 285, 286, 290, 292, 420, 422, 424, 600, 624, 709, 711, 712

Notes on contributors

Dominic Heger received his Diploma in Computer Science from Universität Karlsruhe in 2009. During his studies, he was a visiting research student at Carnegie Mellon University, USA (InterACT scholarship). Since 2009, he is a research assistant

and Ph.D. student at the Cognitive Systems Lab at Karlsruhe Institute of Technology (KIT). His research focus is on innovative methods for the extraction of features from brain signals and machine learning techniques for Brain Computer Interfaces using EEG and fNIRS. He is co-lecturer of the courses "Cognitive Modeling" and "Brain-Computer Interfaces" at KIT.

Reinhard Mutter is a Computer Science student at Karlsruhe Institute of Technology (KIT). Parts of this article, including the experiment recordings, have been performed at the Cognitive Systems Lab within the work for his Bachelor's thesis. His research interests are in the area of Brain Computer Interfacing and machine learning.

Christian Herff studied Computer Science at the Karlsruhe Institute of Technology, fully funded by a scholarship provided by the "Association of German Businesses". During his studies, Christian Herff was a visiting research student at IIT Delhi in India. He acquired his Diploma (Master equivalent) in 2011, which was partly carried out during an invited research stay at the Brain Computer Interface Group, I2R, Singapore. He is currently a research assistant and Ph.D. student at Karlsruhe Institute of Technology at the Cognitive Systems Lab with a research focus on Brain-Computer Interfaces and fNIRS.

Felix Putze has received his Diploma in Computer Science from Universität Karlsruhe. He is a research assistant and Ph.D. student at the Cognitive Systems Lab at Karlsruhe Institute of Technology (KIT). His research focuses on the modeling of cognitive states and cognitive interaction strategies and the processing and interpretation of brain signals for the adaptation of technical systems. He is co-lecturer of the courses "Cognitive Modeling" and "Design and Evaluation of Innovative User Interfaces" at KIT.

Tanja Schultz is a full professor at the Karlsruhe Institute of Technology (KIT) and the founder of the Cognitive Systems Lab. She has also been a research scientist for seven years at Carnegie Mellon University. She received her Ph.D. from KIT in the area of multilingual speech recognition. Within her team she currently works on human-centered technologies and applications for human-computer-interaction and machine mediated human-to-human communication. In 2012, she received the Alcatel-Lucent research award on technical communication and she is currently president of the International Speech Communication Association (ISCA).

References

[1] Picard RW. Affective computing. MIT press; 2000.

[2] D'Mello SK, Craig SD, Witherspoon A, Mcdaniel B, Graesser A. Automatic detection of learners affect from conversational cues. User Modeling and User-Adapted Interaction. 2008;18:45–80.

[3] Nasoz F, Lisetti CL, Vasilakos AV. Affectively intelligent and adaptive car interfaces. Inf Sci. 2010;180:3817–3836.

[4] Heger D, Putze F, Schultz T. An eeg adaptive information system for an empathic robot. Int J Soc Rob. 2011;3: 415–425.

[5] Moore D, Cheng Y, McGrath P, Powell NJ. Collaborative virtual environment technology for people with autism. Focus on Autism and Other Developmental Disabilities. 2005;20:231–243.

[6] Kaliouby Re, Picard R, Baron-Cohen S. Affective computing and autism. Ann NY Acad Sci. 2006;1093:228–248.

[7] Rolls ET. The orbitofrontal cortex and reward. Cerebral cortex. 2000;10:284–294.

[8] LeDoux JE. Emotion circuits in the brain. Annu Rev Neurosci. 2000;23:155–184.

[9] Bush G, Luu P, Posner MI. Cognitive and emotional influences in anterior cingulate cortex. Trends in Cognitive Sci. 2000;4:215–222.

[10] Damasio AR, Grabowski TJ, Bechara A, Damasio H, Ponto LL, Parvizi J, Hichwa RD. Subcortical and cortical brain activity during the feeling of self-generated emotions. Nat Neurosci. 2000;3:1049–1056.

[11] Davidson RJ, Ekman P, Saron CD, Senulis JA, Friesen WV. Approach-withdrawal and cerebral asymmetry: Emotional expression and brain physiology: I. J Personality Soc Psychol. 1990;58:330–341.

[12] Doi H, Nishitani S, Shinohara K. Nirs as a tool for assaying emotional function in the prefrontal cortex. Front Human Neurosci. 2013;7.

[13] Bechara A, Damasio H, Damasio AR. Emotion, decision making and the orbitofrontal cortex. Cerebral cortex. 2000;10:295–307.

[14] Zander TO, Kothe C. Towards passive brain–computer interfaces: applying brain–computer interface technology to human–machine systems in general. J Neural Eng. 2011;8:025005.

[15] Garcia-Molina G, Tsoneva T, Nijholt A. Emotional brain–computer interfaces. Int J of Auton Adapt Commun Syst. 2013;6:9–25.

[16] Sassaroli A, Fantini S. Comment on the modified beerlambert law for cattering media. Phys Med Biol. 2004;49:N255–N257.

[17] Heger D, Mutter R, Herff C, Putze F, Schultz T. "Continuous recognition of affective states by functional near infrared spectroscopy signals", in Affective Computing and Intelligent Interaction (ACII). IEEE. 2013;832–837. ISSN 2156-8103.

[18] Jerritta S, Murugappan M, Nagarajan R, Wan K. "Physiological signals based human emotion recognition: a review," in Signal Processing and its Applications (CSPA), 2011 IEEE 7th International Colloquium on. IEEE. 2011;410–415. ISBN 978-1-61284-414-5.

[19] El Ayadi M, Kamel MS, Karray F. Survey on speech emotion recognition: Features, classification schemes, and databases. Pattern Recognit. 2011;44:572–587.

[20] Lang PJ, Bradley MM, Cuthbert BN. International affective picture system (iaps): Technical manual and affective ratings. Gainesville, FL: Technical report of University of Florida; 1999.

[21] Ekman P, et al. Facial expression and emotion. Am Psycho. 1993;48:384–392.

[22] Russell JA, Mehrabian A. Evidence for a three-factor theory of emotions. J Res Personality. 1977;11:273–294.

[23] Lang P, Bradley MM. The international affective picture system (iaps) in the study of emotion and attention. Handbook of emotion elicitation and assessment. 2007;29–46.

[24] Bradley MM, Lang PJ. The international affective digitized sounds (; iads-2): Affective ratings of sounds and instruction manual. University of Florida, Gainesville, FL: Tech. Rep. B-3; 2007.

[25] Herrmann M, Ehlis A, Fallgatter A. Prefrontal activation through task requirements of emotional induction measured with nirs. Biol Psycho. 2003;64:255–263.

[26] Hoshi Y, Huang J, Kohri S, Iguchi Y, Naya M, Okamoto T, Ono S. Recognition of human emotions from cerebral blood flow changes in the frontal region: A study with event-related near-infrared spectroscopy. J Neuroimaging. 2011;21:e94–e101.

[27] Morinaga K, Akiyoshi J, Matsushita H, Ichioka S, Tanaka Y, Tsuru J, Hanada H. Anticipatory anxiety-induced changes in human lateral prefrontal cortex activity. Biol Psycho. 2007;74:34–38.
[28] Kreplin U, Fairclough SH. Activation of the rostromedial prefrontal cortex during the experience of positive emotion in the context of aesthetic experience. an fnirs study. Front Human Neurosci. 2013;7.
[29] Leon-Carrion J, Damas J, Izzetoglu K, Pourrezai K, Martin-Rodriguez JF, Martin JMBy, Dominguez-Morales MR. Differential time course and intensity of pfc activation for men and women in response to emotional stimuli: a functional near-infrared spectroscopy (fnirs) study. Neurosci Lett. 2006;403:90–95.
[30] Yang H, Zhou Z, Liu Y, Ruan Z, Gong H, Luo Q, Lu Z. Gender difference in hemodynamic responses of prefrontal area to emotional stress by near-infrared spectroscopy. Behav Brain Res. 2007;178:172–176.
[31] Glotzbach E, Mühlberger A, Gschwendtner K, Fallgatter AJ, Pauli P, Herrmann MJ. Prefrontal brain activation during emotional processing: A functional near infrared spectroscopy study (fnirs). The open neuroimaging journal. 2011;5:33–39.
[32] Sitaram R, Zhang H, Guan C, Thulasidas M, Hoshi Y, Ishikawa A, Shimizu K, Birbaumer N. Temporal classification of multichannel near-infrared spectroscopy signals of motor imagery for developing a brain–computer interface. NeuroImage. 2007;34:1416–1427.
[33] Coyle SM, Ward TE, Markham CM. Brain–computer interface using a simplified functional near-infrared spectroscopy system. J Neural Eng. 2007;4:219.
[34] Girouard A. "Adaptive brain-computer interface," in CHI '09 Extended Abstracts on Human Factors in Computing Systems, ser. CHI EA '09. 2009; 3097–3100. doi: 10.1145/1520340.1520436
[35] Ang KK, Guan C, Lee K, Lee JQ, Nioka S, Chance B. A brain-computer interface for mental arithmetic task from singletrial near-infrared spectroscopy brain signals, in Pattern Recognition (ICPR), 20th International Conference on. IEEE. 2010; 3764–3767.
[36] Herff C, Putze F, Heger D, Guan C, Schultz T Speaking mode recognition from functional near infrared spectroscopy, in Engineering in Medicine and Biology Society (EMBC), 2012 Annual International Conference of the IEEE. IEEE. 2012; 1715–1718.
[37] Herff, C, Heger, D, Putze, F, Hennrich, J, Fortmann, O, Schultz, T. Classification of mental tasks in the prefrontal cortex using fnirs, in Engineering in Medicine and Biology Society (EMBC), 2013 35th Annual International Conference of the IEEE. IEEE. 2013; 2160–2163.
[38] Tai K, Chau T. Single-trial classification of nirs signals during emotional induction tasks: towards a corporeal machine interface. J Neuroengineering and Rehabil. 2009;6:39.
[39] Hosseini S, Mano Y, Rostami M, Takahashi M, Sugiura M, Kawashima R. Decoding what one likes or dislikes from single-trial fnirs measurements. Neuroreport. 2011;269–273.
[40] Moghimi S, Kushki A, Power S, Guerguerian AM, Chau T. Automatic detection of a prefrontal cortical response to emotionally rated music using multi-channel near-infrared spectroscopy. J Neural Eng. 2012;9:026022.
[41] Asano H, Sagami T, Ide H. The evaluation of the emotion by near-infrared spectroscopy. Artif Life Rob. 2013;17:452–456.
[42] Amma C, Fischer A, Stein T, Schwameder H, Schultz T. Emotionserkennung auf der Basis von Gangmustern, in Sportinformatik trifft Sporttechnologie, Tagung der dvs-Sektion Sportinformatik, 2010.
[43] Matthews F, Pearlmutter B, Ward T, Soraghan C, Markham C. Hemodynamics for brain-computer interfaces. Signal Processing Magazine, IEEE. 2008;25:87–94.
[44] Cooper R, Selb J, Gagnon L, Phillip D, Schytz H, Iversen H, Ashina M, Boas D. A systematic comparison of motion artifact correction techniques for functional near-infrared spectroscopy. Front Neurosci. 2012;6:147.
[45] Molavi B, Dumont GA. Wavelet-based motion artifact removal for functional near-infrared spectroscopy. Physiol Meas. 2012;33:259.
[46] Khoa TQD, Nakagawa M. Functional near infrared spectroscope for cognition brain tasks by wavelets analysis and neural networks. Int J Biol Med Sci. 2008;1:28–33.
[47] Tsunashima H, Yanagisawa K. Measurement of brain function of car driver using functional near-infrared spectroscopy (fnirs). Comput Intell Neurosci. 2009;2009.
[48] Abibullaev B, An J. Classification of frontal cortex haemodynamic responses during cognitive tasks using wavelet transforms and machine learning algorithms. Med Eng Phys. 2012;34:1394–1410.
[49] Mallat SG. A theory for multiresolution signal decomposition: the wavelet representation. Pattern Analysis and Machine Intelligence, IEEE Transactions on. 1989;11:674–693.
[50] Daubechies I. Ten lectures on wavelets. SIAM. 1992;61:1–357.
[51] Ang KK, Chin ZY, Zhang H, Guan C. Mutual information based selection of optimal spatial–temporal patterns for single-trial eeg based bcis. Pattern Recognit. 2012;45:2137–2144.
[52] Marathe AR, Ries AJ, McDowell K. A novel method for single-trial classification in the face of temporal variability, in Foundations of Augmented Cognition. Springer. 2013; 345–352.
[53] Bradley MM, Sabatinelli D, Lang PJ, Fitzsimmons JR, King W, Desai P. Activation of the visual cortex in motivated attention. Behav Neurosci. 2003;117:369–380.
[54] Rauschecker JP, Scott SK. Maps and streams in the auditory cortex: nonhuman primates illuminate human speech processing. Nat Neurosci. 2009;12:718–724.
[55] Grill-Spector K, Malach R. The human visual cortex. Annu Rev Neurosci. 2004;27:649–677.